

THIS DOCUMENT HAS BEEN APPROVED FOR
PUBLIC RELEASE AND SALE, ITS DISTRIBUTION
IS UNLIMITED.

20

FUEL CELL *7*

RESEARCH & DEVELOPMENT

691340

RESEARCH ON COMPACT
FUEL CELL POWER SUPPLIES

PROGRESS REPORT NUMBER 2

SEPTEMBER 30, 1960 - NOVEMBER 30, 1960

(D)

DDC
RECEIVED
AUG 7 1969
RECEIVED
B

CONTRACT NO. DA-19-129-QM-1705

U. S. ARMY

QUARTERMASTER RESEARCH AND ENGINEERING COMMAND

NATICK, MASSACHUSETTS

This document has been approved
for public release and sale; its
distribution is unlimited

AIRCRAFT ACCESSORY TURBINE DEPARTMENT

GENERAL  ELECTRIC

Reproduced by the
CLEARINGHOUSE
for Federal Scientific & Technical
Information Springfield Va. 22151

54

THIS DOCUMENT HAS BEEN APPROVED FOR
PUBLIC RELEASE AND SALE; ITS DISTRIBUTION
IS UNLIMITED.

RESEARCH ON COMPACT
FUEL CELL POWER SUPPLIES

By

AIRCRAFT ACCESSORY TURBINE DEPARTMENT
FUEL CELL LABORATORY

PROGRESS REPORT NO. 2

SEPTEMBER 30, 1960 - NOVEMBER 30, 1960

For

U. S. ARMY

QUARTERMASTER RESEARCH AND ENGINEERING COMMAND
NATICK, MASSACHUSETTS

AIRCRAFT ACCESSORY TURBINE DEPARTMENT

GENERAL ELECTRIC COMPANY

LYNN, MASSACHUSETTS

TABLE OF CONTENTS

	<u>Page</u>
0.1 Introduction	0-1
0.2 Summary	0-2
0.3 Statement of Work	0-4
0.4 Work Plan	0-6
1.0 Task IA Quantitative Studies of Electrical Losses in Present Cells	1-1
1.1 Separation of Ohmic Losses from Electro-Chemical Irreversibilities	1-1
1.1.1 Separation of Ohmic Electro-Chemical Polarization Losses	1-1
1.2 Magnitude of Ohmic Resistances	1-5
1.2.1 Contact Resistance	1-5
1.2.2 Catalytic Electrode Resistance	1-9
1.2.3 Correlation of Individual Ohmic Resistances	1-13
2.0 Task IB Minimization of Electrolytic Losses	2-1
2.1 Investigate Resin Formulation	2-1
2.2 Effect of Membrane Thickness and Reinforcement on Cell Performance	2-1
2.3 Evaluation of Reinforcing Materials	2-8
3.0 Task IC Minimization of Electronic Losses	3-1
4.0 Task II Internal Generation and Storage of Hydrogen Fuel	4-1

TABLE OF CONTENTS (Cont'd)

5.0	Task III External Generation and Storage of Hydrogen and Oxygen	5-1
5.1	Electrolytic Methods	5-1
5.2	Chemical Methods	5-1
6.0	Appendix A	
	Photographs	6-1

INTRODUCTION

This is a technical progress report of a research program directed toward improvement of the Ion Exchange Membrane Fuel Cell concept. This work is conducted by the General Electric Company under contract No. DA-19-129-QM-1705 with the U.S. Army Quartermaster Research and Engineering Command. The objective of this program is to:

"Initiate research studies to establish those factors which currently contribute the high energy losses of the ion exchange membrane and establish approaches to minimizing such losses to achieve substantially greater power densities per unit weight of cell."

In this series of reports, progress is reported on work directed toward the above objective. In addition, progress is reported on certain related work being conducted at the Aircraft Accessory Turbine Department. This is made possible by virtue of the similarity of the objective of this contract with that of other work being conducted concurrently. The Work Plan for the total work reported is given in section 0.4 of this report. Guidance and approval of the direction of the work under this contract is given by Mr. L.A. Spano - Chief, Advanced Projects Office, Quartermaster Research and Engineering Command, Natick, Massachusetts.

These progress reports are issued on a bi-monthly basis and special summary reports will be issued as indicated. The reader should recognize that this is a progress report covering a particular period of time. The experiments reported are factual, but not necessarily complete, and any conclusions made must be considered tentative until a summary report is issued. Comments and suggestions on these reports are most welcome.

SUMMARY

During the past reporting period of the contracted work, the scheduled investigations by which the internal ohmic losses of the G.E. ion exchange fuel cell were to be quantitatively attributed to various cell components, was nearly complete. A third method of measuring total cell internal resistance has been evaluated and compared with two other methods mentioned in the first Progress Report. The method of measuring the catalyst-layer electrode specific electron resistivity has been improved. A mathematical model for calculating total cell resistance based on cell geometry and the specific electron and ionic resistances of the cell components has been set up for computer solution. An experimental program of evaluating contact resistance between the cell and the current collectors has been set up and nearly completed. Investigations of two types of membrane reinforcements in various thicknesses of ion exchange membrane have led to experimental confirmation of a specific thickness of membrane for minimum ionic resistance for a given amount of reinforcing used.

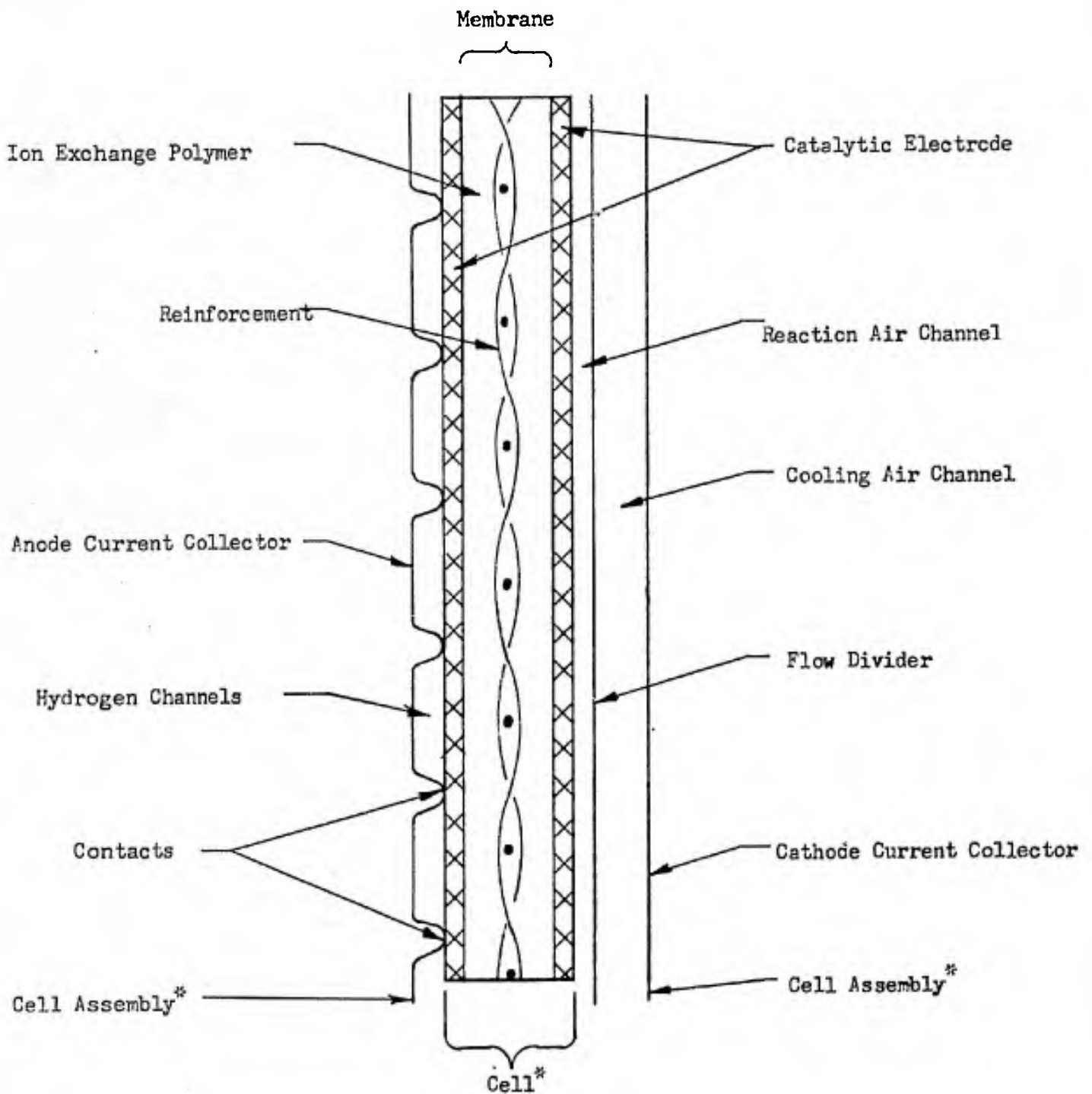
The work is on schedule.

NOMENCLATURE

In future reports, all resistance elements will be referred to by the nomenclature designated in Figure 1 on the next page. The sum of all resistances in the cell assembly will be referred to as the cell assembly resistance. To eliminate confusion, the nomenclature used in the first report, along with the corrected nomenclature, is given below:

<u>Corrected Nomenclature</u>	<u>Progress Report Number 1 Nomenclature</u>
Membrane	Membrane
Cell	Cell
<u>Ion Exchange Polymer</u>	Resin
<u>Catalytic Electrode</u>	Electro-catalyst or catalyst
Current Collector	Fixture or Current Collector
Contact Resistance	Contact Resistance

ION EXCHANGE MEMBRANE CELL NOMENCLATURE



*The word "cell" applies to the combination of electrode layers and ion-exchange membrane, and the phrase "cell assembly" to the cell plus hardware.

Figure 1.

0.3 STATEMENT OF WORK

A. SCOPE:

The Contractor shall, commencing on 3 October 1960 and continuing through 2 October 1961, furnish necessary services, labor, materials, tools, equipment and supplies, and will furnish his best efforts to do what is deemed necessary to:

Initiate research studies to establish those factors which currently contribute the high energy losses of the ion exchange membrane and establish approaches to minimizing such losses to achieve substantially greater power densities per unit weight of cell. The principal effort under this contract should include but not be limited to a study of the factors that impede the conduction of electronic and ionic charges. Investigation of resins, membrane and catalyst formulations and their incorporation into a cell should be conducted to achieve maximum performance.

B. REPORTS:

Reports shall be submitted in accordance with the following:

1. The Contractor shall submit ten (10) copies of bi-monthly reports within fifteen (15) days following the end of each reporting period, indicating progress of work to date and significant developments. These quarterly reports shall include:
 - a. An estimate of the percentage of work completed to date.
 - b. An estimate of the percentage of costs incurred to date.
 - c. A statement that to the contractor's best knowledge the funds remaining unexpended are sufficient to complete the work called for by the contract, or a revised estimate setting forth the costs required to complete the contract and the reason(s) for the contemplated excess.

REPORTS (Cont'd)

2. Upon completion or termination of the contract, the contractor shall furnish fifty (50) copies of a complete final report or summary report which shall consolidate all findings, notes, data, computations, test procedures, evaluation of all data, test results, principles and techniques relative to the objective indicated herein. The contractor shall include specific conclusions and recommendations concerning work done and detailed information and recommendations relative to further work that may be required. All reports shall be identified with Project No. 7X80-01-New. The final report shall be submitted within thirty (30) days after the expiration or termination date of the contract. Reports shall be of a paper bound brochure type using commercially available bond paper. All reports shall be submitted to the responsible Project Officer, Chemicals & Plastics Division, HQ QMR&E Center, Natick, Massachusetts.

PRIORITY RATING: DD C9E CERTIFIED UNDER DMS REGULATION #1 IS
ASSIGNED TO THIS CONTRACT.

PLACE OF PERFORMANCE: Contractor's plant, West Lynn, Massachusetts.

0.4

WORK PLAN

REGULATED, COMPACT FUEL CELL POWER SUPPLIES

General Objective

Conduct a research and development program to achieve the capability of designing compact, lightweight and reliable, regulated fuel cell power supplies.

Research Approach

Task I

Studies of Contributions to and efforts to minimize electronic and ion impedances.

- A. Quantitative studies of contributions to electrical losses in present cells.
 - 1. Separate ohmic losses from electrochemical irreversibilities by use of an adaptation of the Kordesch-Marko bridge and other electronic techniques.
 - 2. Determine magnitude of various contributions to ohmic impedance by independent measurements of electrode-layer resistance, current-collector resistance, contact resistance, and electrolytic conductivity of the membranes. Establish apparent ohmic resistance attributable to electrolytic conductivity of the membranes by other methods, including multi-frequency A.C. bridge measurements and driven-cell D.C. resistance with two hydrogen electrodes.
- B. Minimization of electrolytic conductance losses.
 - 1. Investigate ion exchange resin formulations with varying exchange capacities, ionization constants and water content with regard to their effect on cell performance.
 - 2. Investigate the effect on cell performance of membrane thickness along with varying the amount and distribution of resin and reinforcing material.

3. Evaluate various reinforcing materials from the standpoint of cell performance, strength, compatibility, and ease of membrane manufacture.
- C. Minimization of electronic losses.
1. Investigation of catalyst impregnated carbon electrodes to minimize electrode layer resistance.
 2. Evaluate various carbon blacks with different catalyst loadings and physical properties with regard to cell performance and life.

Task II

Study of the internal generation and storage of hydrogen fuel

- A. Studies at the Electronics Laboratory, HMED, Syracuse, of palladium and other absorbents.
- B. Provision of data by the AAT Laboratory on the electrolysis characteristics of membrane fuel cells, including details of supplying the water required for such operation.

Task III

Study of the external generation and storage of hydrogen and oxygen

- A. Electrolytic methods. Engineering work leading to the development of a prototype model of a small high pressure electrolyzer. The initial design concept is that of a compartmented vessel for simultaneous generation and containment of hydrogen and oxygen in quantities sufficient for operation of a fuel cell for a specified duty cycle. Included will be studies of pressure reduction methods including minimum weight regulators of conventional design.
- B. Chemical Methods. Studies of various chemical systems for minimum volume and cost hydrogen generators. The size will be set by the required duty cycle. Noxious reaction products are to be avoided. Feasibility of the process using the best of the chemical system(s) will be demonstrated by constructing a laboratory model generator including pressure regulators as required.

1.0 Task 1A - Quantitative Studies of Electrical Losses in Present Cells

1.1 Separation of Ohmic Losses from Electro-Chemical Irreversibilities.

Progress Report Number 1 described two methods for determining the internal ohmic resistance of a fuel cell assembly. A third approximate method, which involves driving a cell with hydrogen gas present at both electrodes, is described in this report section. This method was also used to determine the irreversibility of the hydrogen electrode and indicated the magnitude of error involved if resistances are determined by this method without correcting for the hydrogen electrode polarization. Task I A1 of the Work Statement has been completed.

1.1.1 Separation of Ohmic and Electrochemical Polarization Losses

The Kordesch-Marko bridge was used to separate the ohmic resistance from the electrochemical polarizations of all experimental cells made to date. The reproducibility of these results was found to be almost identical with that reported in Progress Report Number 1.

The following Table I lists the results of resistance measurements by the Kordesch-Marko and the a.c. bridges for twenty-two cells.

TABLE I

Comparison of Cell Resistance using Kordesch-Marko and a.c. bridges.

<u>AC Bridge Resistance (ohm-cm²)</u>	<u>Kordesch Marko (ohms-cm²)</u>	<u>Percent Deviation</u>
2.89	2.72	+6.3
2.59	2.42	+7.0
2.11	2.03	+4.0
1.98	2.04	-3.0
9.54	9.50	+0.5
14.4	14.15	+2.0
3.30	2.78	+18.7
2.47	2.75	-10.0
2.44	2.39	+2.1
2.44	2.46	-0.8
1.98	2.01	-1.5
2.01	1.69	19.0
2.84	2.64	+7.6
6.95	6.25	+11.2

TABLE I (Cont'd)

<u>AC Bridge Resistance</u> (ohm-cm ²)	<u>Kordesch-Marko</u> (ohms-cm ²)	<u>Percent Deviation</u>
4.46	4.23	+5.4
3.31	3.59	-7.8
2.86	3.22	-11.1
2.58	2.44	+5.8
2.87	2.93	-2.0
2.53	2.53	0.0
6.20	6.53	-5.1
3.09	3.15	-1.9
		Av. Deviation $\pm 6\%$

The ohmic resistances of the experimental cells were also determined by direct measurement with a General Radio 50A 1000 cycle a.c. bridge. The bridge itself is only readable to $\pm 10\%$ and was used as a check on the Kordesch-Marko. The Kordesch-Marko bridge resistances were well within the readability of the a.c. bridge values and an average of all values showed a deviation of $\pm 6\%$ between the two methods. Due to its greater accuracy, the Kordesch-Marko technique has been adopted as the standard for the accurate determination of cell assembly resistance.

In the normal operation of the Kordesch-Marko bridge, a cell was driven by the bridge, while simultaneously converting hydrogen and oxygen to electricity and supplying power of its own of the same polarity as the bridge power. A further technique for determining the cell resistance, as well as the hydrogen polarization, was evaluated. It involves driving the fuel cell with the Kordesch-Marko bridge with hydrogen present at both catalytic electrodes. Thus, the cell is unable to supply power of its own, and the voltage drop measured across the cell is due to the ohmic resistance of the cell and the electrochemical polarization of the hydrogen at the two electrodes. Also the cell is operated on the Kordesch-Marko circuit in the same manner as with hydrogen and oxygen. Voltage and current readings were taken exactly the same as described in Progress Report Number 1. However, in this case "Pot B" measures the voltage drop due to the polarization at the two hydrogen electrodes, while "Pot A" measures the sum of the ohmic impedance plus the hydrogen polarization. Here one hydrogen electrode was operating in the normal manner while the other was running in reverse.

By using hydrogen gas at both electrodes, a check on the operation of the Kordesch-Marko bridge was obtained. It is generally known that the hydrogen electrode is practically reversible. Therefore, when running on the Marko bridge, the voltage curve running with interrupted current should be close to zero. This was found in fact to be true, with only a slight polarization due to the hydrogen electrode.

Cell #57 was operated on the Kordesch-Marko bridge with hydrogen and oxygen at the respective electrodes. From this the total ohmic impedance of the cell was determined as well as the electrochemical polarization of the hydrogen and oxygen electrodes. The ohmic impedance value obtained was 3.02 ohm-cm^2 . This same cell was then operated with hydrogen at both electrodes. The ohmic impedance was again found to be 3.02 ohm-cm^2 , and the electrochemical polarization of the two hydrogen electrodes was found to be very small. Figure 2 shows a plot of the various Kordesch-Marko curves obtained on Cell #57.

As can be seen in Figure 2, based on a theoretical cell voltage of 1.23, the sum of the electrochemical polarization at the two hydrogen electrodes is only $\frac{0.005}{0.02\text{A/cm}^2}$ or 0.25 ohm-cm^2 . In contrast, the sum of the polarizations at the hydrogen plus the oxygen electrodes is $\frac{0.389}{.02\text{A/cm}^2}$ or 19.45 ohm-cm^2 at 20 milliamps per cm^2 . In each case the resistance of the cell assembly was 3.02 ohm-cm^2 . At higher current densities, the apparent ohm-cm^2 values of electrode polarizations drop while resistance remains the same.

If, as is frequently done by other investigators, the ohmic resistance is determined by driving a cell with hydrogen at both electrodes using a d.c source and assigning the total induced d.c. voltage drop across the cell to the ohmic resistance (assuming zero hydrogen polarization losses), the error involved would be less than 10% which, for most cases, is acceptable.

A complete separation and determination of the electrochemical polarization and total ohmic impedance losses within the cell assembly have been completed. The methods have been shown to be accurate and reliable within the scope of this work. No further discussion of methods for the separation of ohmic losses from electrochemical irreversibilities, or the determination of such losses, will be undertaken. The Kordesch-Marko technique will be used as the tool for cell assembly resistance determinations in future work and obtained data by this technique will be reported.

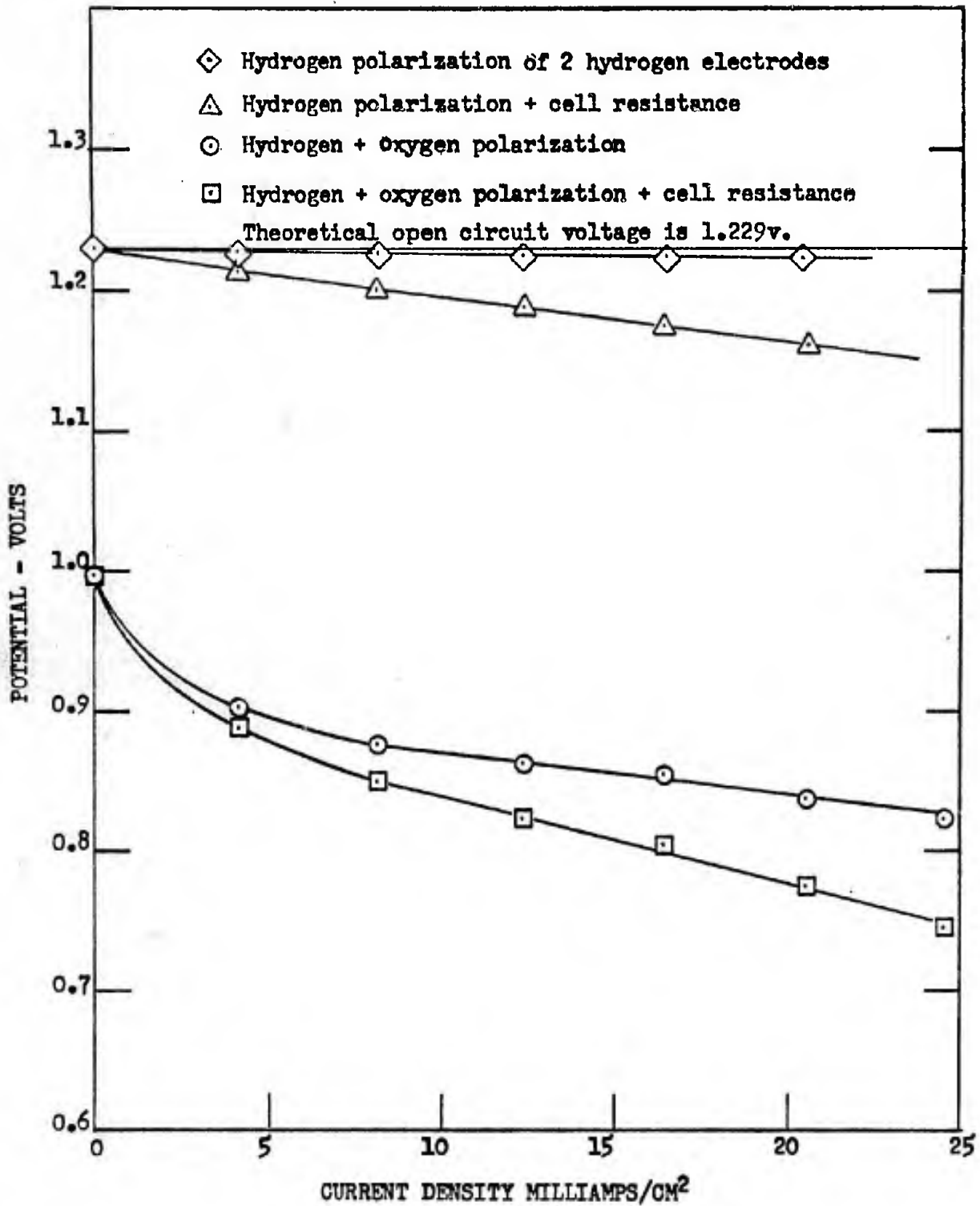


FIG 2 HYDROGEN, OXYGEN POLARIZATION AND INTERNAL RESISTANCE OBTAINED FROM ELECTRICAL INTERRUPTOR MEASUREMENTS 1-4

1.2 Magnitude of Ohmic Resistances

Methods for determining ion exchange polymer resistance, catalytic electrode resistance, and membrane resistance were described in Progress Report Number 1. This section describes a method for determining the magnitude of the contact resistance as well as a modification of the catalytic electrode-layer resistance measurement. Also described is a computer program which has been established to correlate the individual ohmic resistances with cell assembly resistance. The only remaining work elements in Task I A2 of the Work Statement are to show good correspondence between the computer program and experimental data, and then to calculate via the computer a parametric study of factors affecting internal cell resistance.

1.2.1 Contact Resistance

Usually when current flows from one conducting body to another in contact with it, a voltage drop is suffered as the current passes through the contact area. The cause can be threefold:

- A. Films, either organic or oxide, which are only partially conducting.
- B. The roughness of the contacts, which causes the contacts to touch only at a fraction of the total available contact area, thus restricting the current through small "tubes" where energy dissipation occurs.
- C. The electrical properties of the contacts and their geometric relationship.

Most contact resistance will be a function of:

- A. Type of metal.
- B. The area of contact.
- C. The contact pressure.
- D. The perimeter of the contact area.
- E. Experimental environment (humidity, dust, carbon monoxide, etc.).

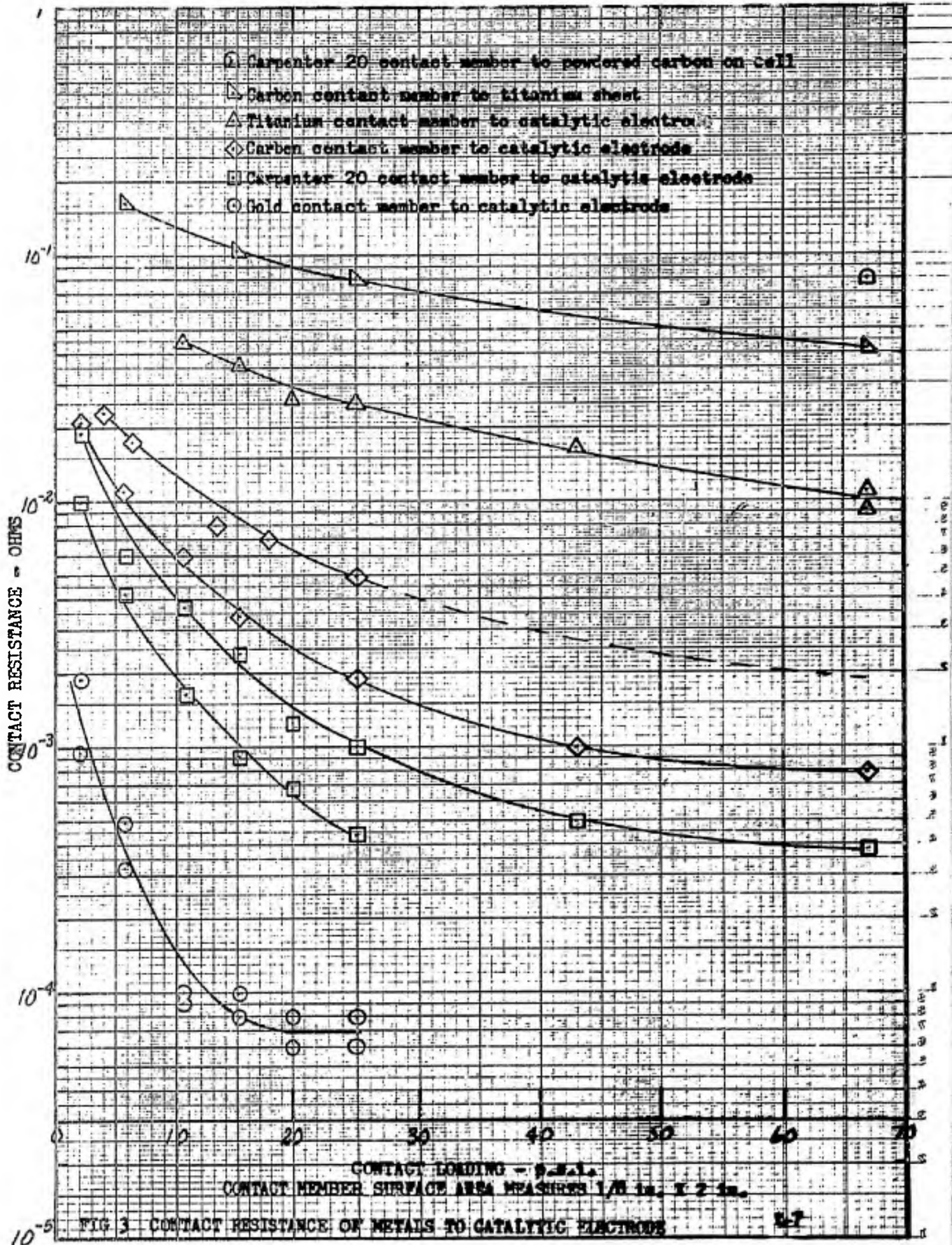
A study has been undertaken to determine the contact resistance of various metals to the catalytic electrode of a typical cell. The metals tested were pure titanium, Carpenter 20 Stainless Steel, carbon (bound with cold tar), and gold plate.

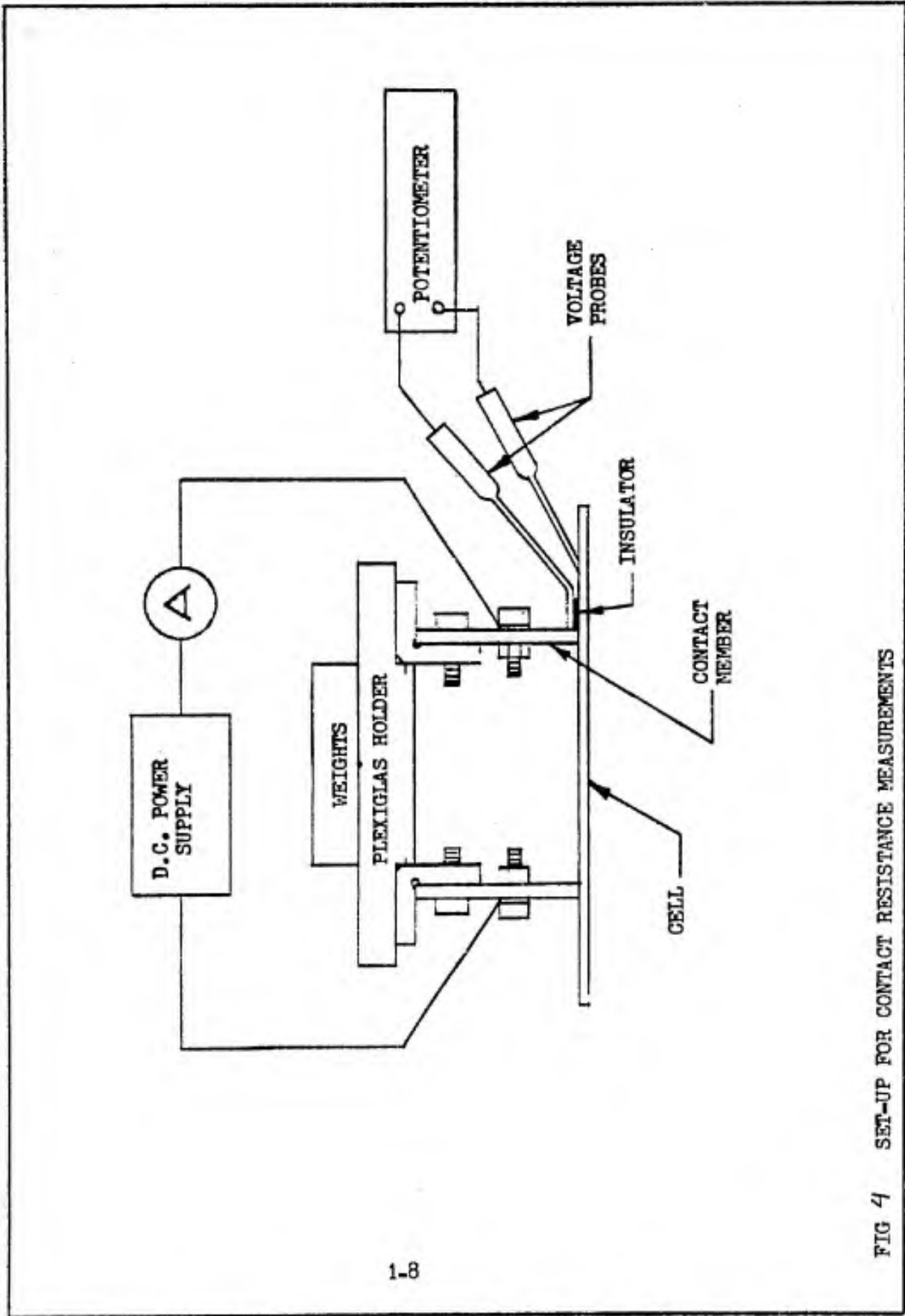
The first three could be commonly used as current collectors. Gold plate is used for current collectors in experimental studies because it is believed to have low contact resistance since it does not form oxide films at ordinary temperatures and is relatively malleable.

The apparatus to measure contact resistance is shown in Figure 4. It consists of an insulating plexiglas support to which two holders are attached. The holders carry the solid contact members whose contacting areas simulate the contacts in the actual current collectors used in previous studies. The fixture was made so that contacting members of different materials and thicknesses could be interchanged.

The test fixture was placed on a strip of cell with the width exactly equal to the width of the contact members. Current was supplied by a d.c. power supply through the contact members, thence through the contact area and along the catalytic electrode. The voltage drop across the contact area was measured by placing a probe against the contact member as close as possible to the catalytic electrode (to avoid including the very slight voltage drop through a length of the solid contact member). The member probe was held away from the catalytic electrode by a .002 inch thick strip of "mylar". Another probe was placed on the "overhung" catalytic electrode and the voltage drop measured on a potentiometer. It was noted that if the width of the cell was exactly equal to the width of the contact members, an equipotential field existed on the overhung portion of the catalytic-layer electrode, where there was no current flowing along the electrode layer. Hence the potential on the "overhang" closely approximates the potential of the catalytic layer under the solid contact member.

Care was taken to machine the fixture with supporting surfaces flat and parallel so that the surfaces of the contacting members were in the same plane. The fixture and cell were placed for testing on a flat granite surface plate which had been leveled by shimming. Even with the precautions mentioned above, care was necessary in loading the fixture uniformly with weights to obtain equal pressure. Occasionally some discrepancy was noted between the contact resistance from the cell to one contact member and the similar member on the other side of the fixture, indicating non-uniform pressure distribution. The non-uniform pressure was assumed to be caused by high spots in the catalyst surface which could have been introduced in manufacture. Consequently the test was run by shifting the weights along the holding fixture until the contact resistance was constant along the length of the contacting area as well as from one member to the other.





1.8

FIG 4 SET-UP FOR CONTACT RESISTANCE MEASUREMENTS

The contacting members were then assumed to transmit an "average" pressure as indicated by the weights and the apparent contacting surface area of the members.

When encountered, this "averaging" problem was not serious, even at the higher pressures where the compliance of the plastic membrane helped in the equalization process.

The first part of this study involved testing different contact members of the same contact surface area and geometry under various pressures. Figure 3 shows the data plotted. Note that the contact resistance was not reduced to a contact resistivity, since the effect of contact area on contact resistance is not known. Even if it is assumed that contact resistance is directly related to surface area, the values for gold or Carpenter 20 Stainless Steel have negligible contribution to the total cell resistance of a typical cell. On the other hand, titanium and carbon show very high values.

This approach of measuring contact resistance has shown itself to be satisfactory for the purposes of this investigation. Future work will be conducted using members of varying area, and members of constant area, but varying perimeters, to find the effect of surface area and perimeter on contact resistance.

1.2.2 Catalytic Electrode Resistance

A slight modification has been made in the method of measuring the catalytic-layer electrode resistance. The apparatus, described in Progress Report Number 1, involved the use of 0.5 inch wide electrodes seating against a 0.5 inch wide cell setup. It has since been found that this method is very sensitive to small discontinuities in the catalytic electrode and often results in unrealistically high resistances. The modified method utilizes the gold plated 2.0 inch wide fixtures described above for the measurement of contact resistance. A cell strip 2.0 inch wide is employed where the probability of incurring discontinuity across the entire 2.0 inch width is slight. The method of plotting catalytic electrode length against resistance is still used where the electrode spacings are preset at 0.5 inch, 1.0 inch, 2.0 inch, 3.0 inch, and 4.0 inch. However, it is now possible to directly measure the contact resistance which in the case of gold versus catalysts "A" (Pt.) and "B" (Pd.) is insignificant.

The catalytic electrode resistances were determined on ten cells with hydrogen catalyst loadings of 0.0375 gram of palladium black per square inch, and oxygen catalyst loadings of 0.0375 of platinum black added to 0.0375 grams of palladium black per square inch. The hydrogen catalytic electrode resistance averaged 0.48 ohms/"square"* with an average deviation of ± 0.13 ohms/"square". The oxygen catalytic electrode resistance averaged 0.41 ohms per "square"* with an average deviation of ± 0.08 ohms/"square". This data is shown in Table II . These values compare to 0.45 ohms/"square" and 0.39 ohms/"square", respectively, determined on a single cell and reported in Progress Report Number 1. Two cells were made in which these loadings were doubled, and resistances of approximately one half were obtained as expected.

It should be noted that the above results were obtained on cells where a proprietary procedure for uniformly distributing the catalytic electrode on the membrane is used. Determinations made on cells which had the catalytic electrode applied by an older, non-uniform method showed slightly higher resistances with deviations of 0.60 ohms/square.

The percent of total cell resistance attributable to the catalytic electrodes is shown in Table III Page 1-12. These results were obtained by comparing the cell assembly resistance obtained by the Kordesch-Marko bridge with the membrane resistance obtained on flat, parallel gold-plated current collectors by an a.c. bridge (Progress Report Number 1, page 2-16). Since the contact resistance of gold versus the cell has been previously shown to be negligible and the current collector resistance is also negligible, the difference between the Kordesch-Marko resistance and membrane resistance is directly attributable to the catalytic electrode resistance.

* Square - a specific resistance divided by an unknown thickness dimension. (Ref. - Report #1 Page 2-10)

TABLE II

<u>Cell Number</u>	<u>Hydrogen Catalyst</u>	<u>Catalytic Electrode Resistances</u>		<u>Oxygen Catalyst</u>
	Resistance (ohms/"square")	Deviation from mean <u> %</u>	Resistance (ohms/"square")	Deviation from mean <u> %</u>
E 9	0.58	0.10	0.46	0.055
E 10	0.75	0.27	0.43	0.025
E 12	0.62	0.14	0.44	0.035
E 13	0.65	0.17	0.42	0.015
E 14	0.36	0.08	0.42	0.015
E 56	0.28	0.20	0.33	0.075
E 58	0.29	0.19	0.18	0.245
E 59	0.43	0.05	0.58	0.175
E 60	0.45	0.03	0.39	0.015
E 61	0.40	0.08	0.40	0.015
Average	0.48	0.13	0.405	.075

Thus this difference gives us a way of finding the contribution of the electrode layer to the total cell resistance when it is with a ribbed current collector. The cells listed in Table III Section 1A, have identical catalyst loadings of 0.0375 g./in² of palladium catalyst and 0.0375 g./in² of mixed oxygen catalyst (palladium and platinum) on the membrane. This data was obtained on paralleled-ribbed-current collectors where the ribs were 0.1 inch wide by 3.5 inch in electrode area.

The cells listed in Section B had various percentages of platinum black on the oxygen side replaced by carbon black. There was no palladium black on the oxygen side in these cells.

Thus, with the particular current collector geometry described above, cells with hydrogen catalytic electrode resistances of 0.49 ohms."square"* have cell assembly resistances of which an average of 16% is attributable to the catalytic electrode. This figure of 16% is obtained from the difference between the two values of resistance, one as a cell assembly resistance, the other, where effectively, only the membrane resistance was measured.

A correlation of the catalytic electrode resistance in ohms per "square"*, the current collector geometry, and the actual percentage of cell assembly resistance, attributable to catalytic electrode resistance, is presently being investigated. This correlation will be more completely described in the following section.

TABLE III

Cell No.	Cell Assembly Resistance ** (OHM-CM ²)	Membrane Resistance*** (OHM- CM ²)	Percent Catalyst Contribution to Cell Resistance
Section A			
9	2.72	2.16	20.6
10	2.42	2.10	13.2
11	2.03	1.43	29.8
12	2.04	1.61	21.0
13	9.50	8.33	12.3
14	14.15	10.70	25.0
45	2.78	2.53	9.0
56	2.76	2.29	16.7
57	3.02	2.68	11.3
58	2.68	2.22	17.1
59	2.46	2.16	12.2
60	2.01	1.63	3.6
		Average	<u>16.6%</u>

* Square - a specific resistance divided by an unknown thickness dimension.

** Measured with the Kordesch-Marko bridge.

*** Measured with an a.c. bridge.

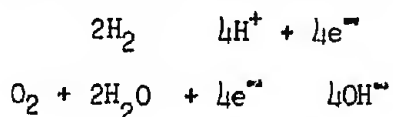
TABLE III (Cont'd.)

<u>Cell No.</u>	<u>Cell Assembly Resistance** (OHM-CM²)</u>	<u>Membrane Resistance*** (OHM-CM²)</u>	<u>Percent Catalyst Contribution to Cell Resistance</u>
61	1.69	Section A (Cont'd.) 1.63 Average	<u>3.6</u> <u>16.6%</u>
Section B			
SC 19 (100%*)	6.53	3.66	44.0
SC 14 (80%*)	9.78	3.16	67.5
SC 37 (27%*)	3.50	2.42	32.0
SC 22 (0%*)	3.15	2.62	16.8

- * Percent by weight catalyst A (Pt.) replaced by carbon on the oxygen side.
 ** Measured with the Kordesch-Marko bridge.
 *** Measured with an a.c. bridge.

1.2.3 Correlation of Individual Ohmic Resistances

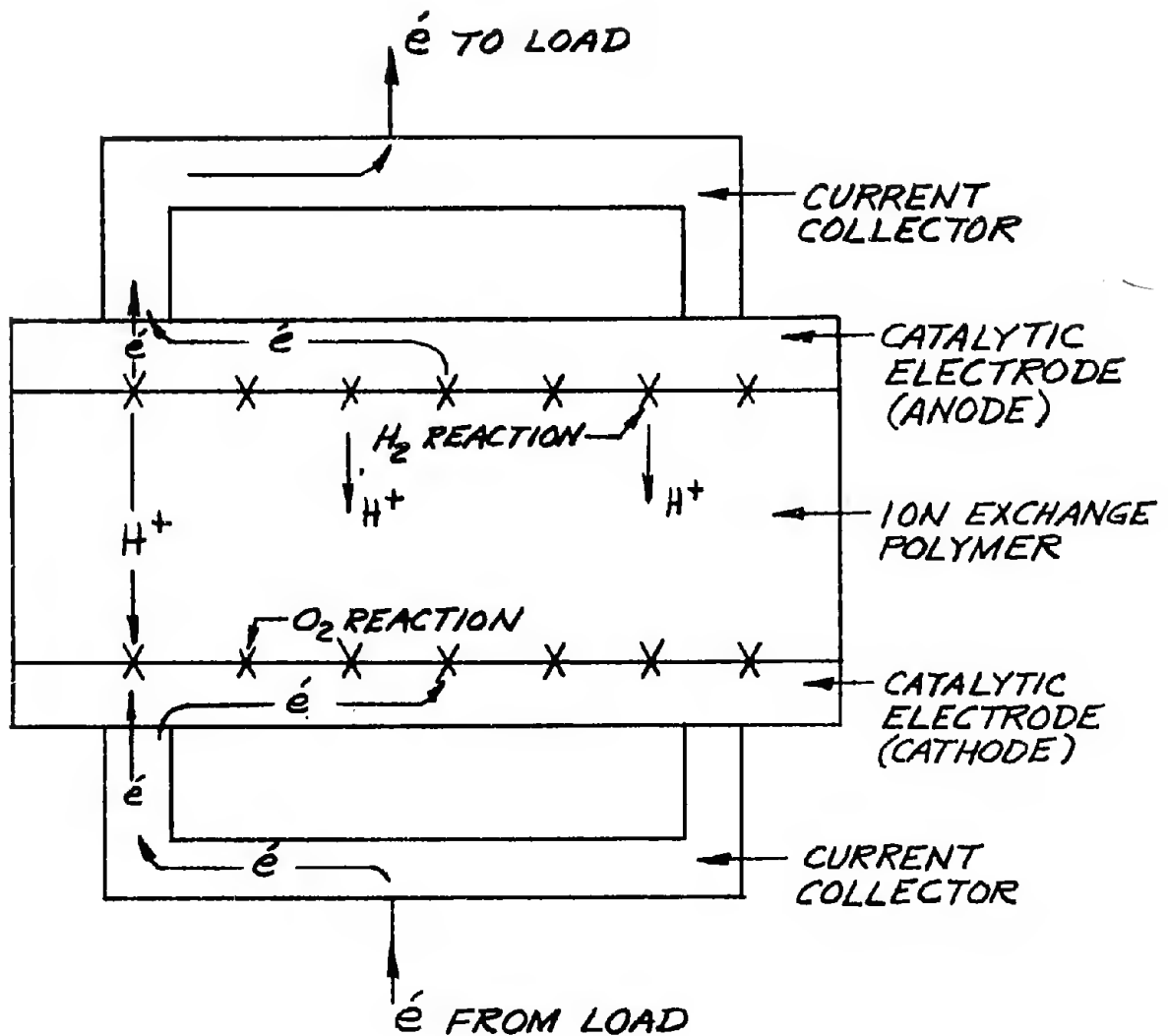
In order to understand the contributions of component resistances to overall cell resistance, the general operation of a fuel cell is summarized. Referring to the model on Page 1-14, it is seen that the reactions of oxygen and hydrogen take place as:



The reactions take place at the interface between catalytic electrode and ion exchange polymer, and upon reacting, hydrogen ions (protons) are exchanged through the ion exchange polymer to the cathode and combine there with OH⁻ ions to form water.

The resistance to ion and current flow in the cell arise from the following factors:

- A. The resistance to proton flow through the ion exchange polymer. This depends on the nature of the polymer and the type and amount of non-conducting reinforcing material used to strengthen the polymer.



MODEL - ION EXCHANGE FUEL CELL

- B. The electrical contact resistance between the catalytic electrode and current collector.
- C. The electrical resistance of the current collector.
- D. The electrical resistance of the catalyst layer. This comprises a unique problem and is discussed below.

From the model on Page 1-14, it can be seen that before a reaction can take place at the cathode, an electron must move from the current collector to the reaction site. In the case where a reaction site is halfway between adjacent contact points, the path of the electron is longest. On the other hand, the electron which travels to a site directly opposite a collector contact travels a short distance and, therefore, encounters little resistance. The total catalytic resistance is, then, the sum of all the resistances encountered by all the electrons flowing and will depend on the catalyst type and geometry and the geometry of the current collector (spacing between contacts, and size of contacts).

If the appropriate resistivities of all components are measured, and the total geometry of the cell is specified, then a total ohmic resistance can be calculated, preferably on a digital computer, making provision for integrating resistance through the catalytic electrode.

Enough information has been obtained on the resistivities of all components to allow a computation of overall cell resistance and comparison to measured cell resistance. One may go a step further and study the effects of varying cell geometry to find areas where total cell resistance may be reduced.

The effective resistance of the membrane is calculated by using numerical methods to solve Laplace's Equation. The numerical solution methods are part of a standard program suitable for use on the IBM 704 computer. The program was compiled to solve network problems which occur frequently.

The adaptability of the program to the problem of estimating effective membrane resistance may be judged, to some extent, by reviewing the type of problem the program is capable of solving. Also, in the future, more experimental comparisons with computer results will be furnished.

A. One-Dimensional Considerations

Consider the flow of current in a conducting bar segment where the ends of the segment are held at potentials V_i and V_j , respectively. (See Figure 5) The governing equation is, of course,
 $V_i - V_j = IR$

Where the resistance R , of the segment is found from

$$R_1 = \rho_1 \frac{\Delta X_1}{A_1} \quad (2)$$

ρ_1 = resistance in ohm - cm.

X_1 = length - cm

A_1 = current flow area - cm^2

The potential (V_1) of a node in the middle of the segment is given by either

$$V_i - V_1 = I \cdot \rho_1 \frac{X_{i-1}}{A_1} \quad (3)$$

$$V_1 - V_j = I \cdot \rho_1 \frac{X_{1-j}}{A_1} \quad (4)$$

Now consider a system where the foregoing segment is adjacent to a second segment. (Figure 6)

The equations for the second segment, subscript 2, correspond to the equations for the first segment.

$$V_j - V_k = I_2 R_2 \quad (5)$$

$$R_2 = \rho_2 \frac{\Delta X_2}{A_2} \quad (6)$$

$$V_j - V_2 = I_2 \rho_2 \frac{X_{j-2}}{A_2} \quad (7)$$

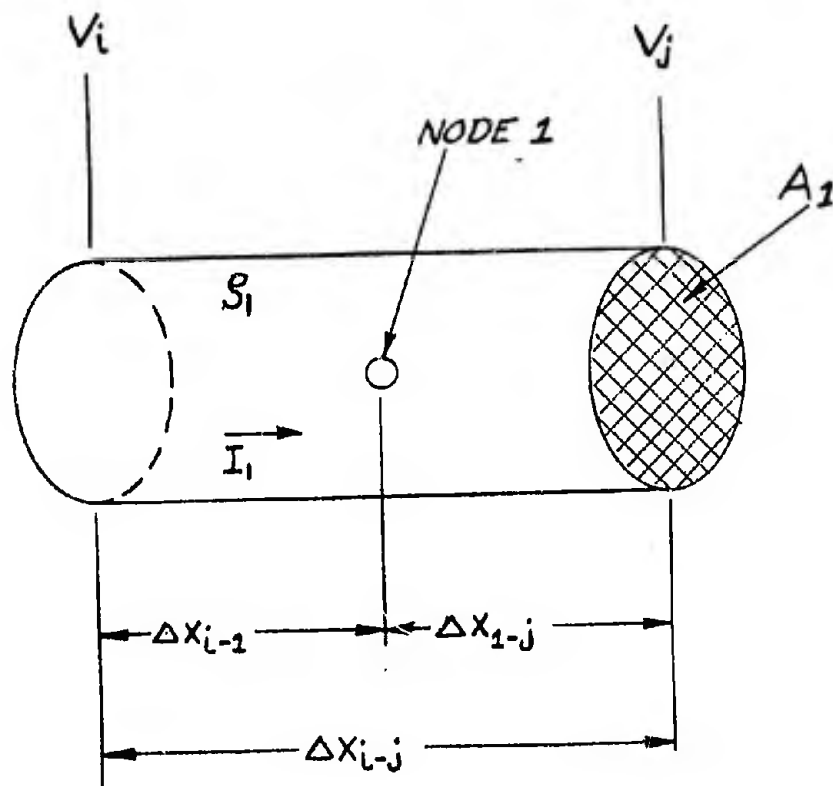


FIGURE 5
ONE-DIMENSIONAL MODEL OF FLUX-TUBE ELEMENT

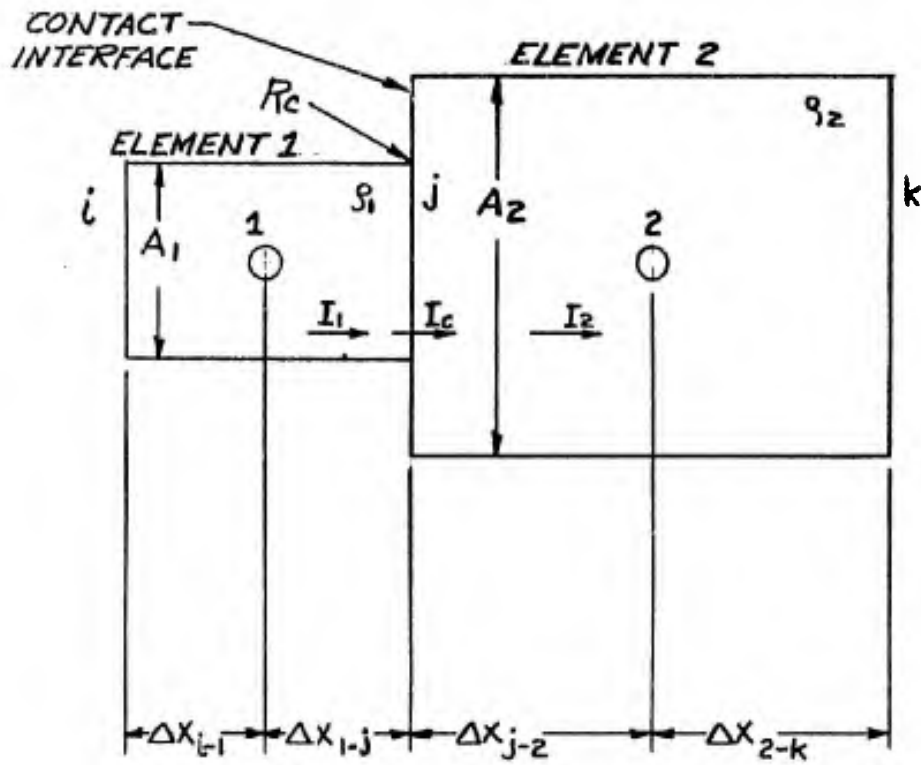


FIGURE 6
TWO-ELEMENT MODEL

$$V_2 - V_k = I_2 \int_2 \frac{X_{2-k}}{A_2} \quad (8)$$

Note that the j-face of node "1" will have the same potential as the j-face of node "2" unless there is a contact resistance, R_c .

If there is no contact resistance the equation relating the potentials of nodes 1 and 2 is found by combining Equations 4 and 7.

$$V_1 - V_2 = I_1 \int_1 \frac{X_{1-j}}{A_1} + I_2 \int_2 \frac{X_{j-2}}{A_2} \quad (9)$$

The presence of a contact resistance simply adds an $I_c \frac{R_c}{A_c}$ term to the right side of Equation 9, i.e., a potential drop.

$$\begin{aligned} V_1 - V_2 = & I_1 \int_1 \frac{X_{1-j}}{A_1} + I_{c1-2} \frac{R_{c1-2}}{A_{c1-2}} \\ & + I_2 \int_2 \frac{X_{j-2}}{A_2} \end{aligned} \quad (10)$$

The contact resistance R_c has units of ohm-cm².

During steady state operation $I_1 = I_{c1-2} = I_2 = I_{1-2}$ and Equation 10 reads

$$V_1 - V_2 = I_{1-2} \left[\int_1 \frac{\Delta X_{1-j}}{A_1} + \frac{R_{c1-2}}{A_{c1-2}} + \int_2 \frac{\Delta X_{j-2}}{A_2} \right] \quad (11)$$

or

$$V_1 - V_2 = I_{1-2} \bar{R}_{1-2} \quad (12)$$

where \bar{R}_{1-2} is the total resistance the current sees in going from node 1 to node 2

$$\bar{R}_{1-2} = \int_1 \frac{\Delta X_{1-j}}{A_1} + \frac{R_{c1-2}}{A_{c1-2}} + \int_2 \frac{\Delta X_{j-2}}{A_2} \quad (13)$$

Let us now consider an entire rod containing N segments or nodes (Figure 7). It follows from Kirchoff's Law that, in steady state, the net current flow into each node is zero.

For example, for node q.

$$I_{p-q} + I_{q-r} = 0 \quad (14)$$

or

$$\frac{V_p - V_q}{R_{pq}} = \frac{V_q - V_r}{R_{qr}} \quad (15)$$

Equation 15 is written for convenience as

$$\frac{1}{R_{pq}} V_p - \left(\frac{1}{R_{pq}} + \frac{1}{R_{qr}} \right) V_q + \frac{1}{R_{qr}} V_r = 0 \quad (16)$$

If the potentials at each end of the rod are specified we can write N equations of the form of Equation 16 for the N nodes, and thus arrive at an N x N matrix with the N unknowns, i.e. the N node potentials. This matrix we can solve in any number of ways.

B. Two-Dimensional Problems

Two dimensional problems are more complex only in the sense that more variables are present in each working equation. The theory is unchanged. Consider node X in the system shown in Figure 8. The net current flow to node X in steady state must be zero.

$$I_{1-x} + I_{2-x} + I_{3-x} + I_{4-x} = 0 \quad (17)$$

This consideration leads to

$$\frac{V_1 - V_x}{R_{1-x}} + \frac{V_2 - V_x}{R_{2-x}} + \frac{V_3 - V_x}{R_{3-x}} + \frac{V_4 - V_x}{R_{4-x}} = 0 \quad (18)$$

or

$$\frac{1}{R_{1-x}} V_1 + \frac{1}{R_{2-x}} V_2 + \frac{1}{R_{3-x}} V_3 + \frac{1}{R_{4-x}} V_4$$

$$- \left(\frac{1}{R_{1-x}} + \frac{1}{R_{2-x}} + \frac{1}{R_{3-x}} + \frac{1}{R_{4-x}} \right) V_x = 0 \quad (19)$$

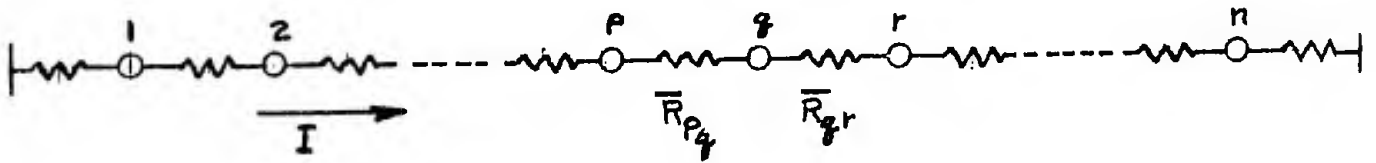
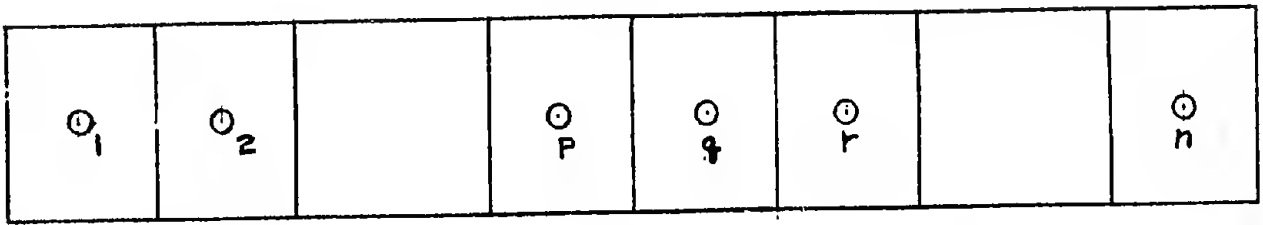


FIGURE 7
GENERALIZED N-NODE PROBLEM

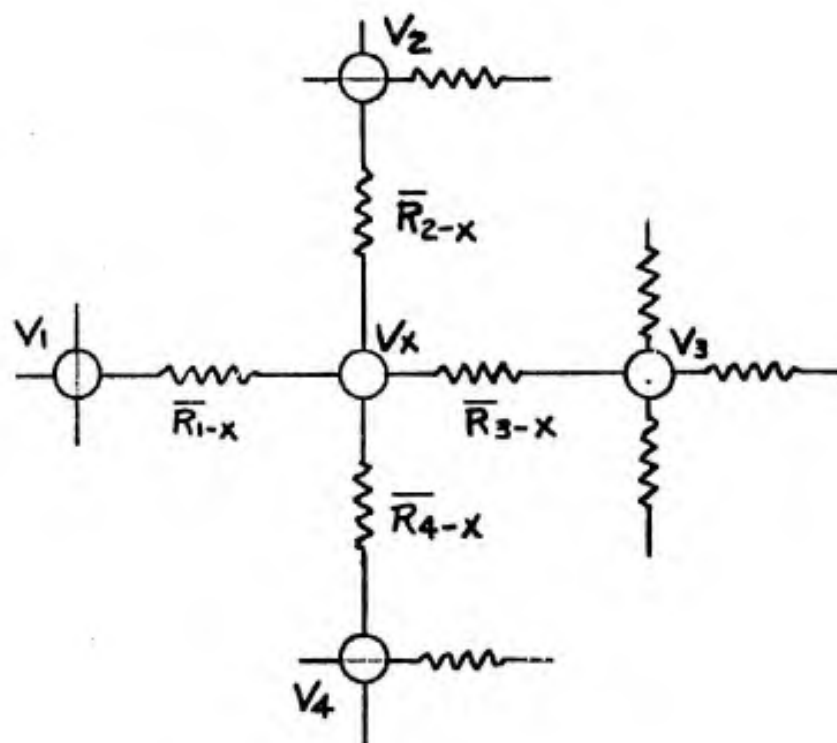


FIGURE 8
THE TWO-DIMENSIONAL PROBLEM

If the total system contains M nodes we can write the M x M matrix, which is necessary to solve the problem, by using Equation 19.

C. Boundary Considerations

The effect of a boundary is incorporated as follows:

Consider the end of a rod, Figure 9. We write an equation of the form of Equation 16 for node 1.

$$\frac{1}{R_{0-1}} V_0 - \left(\frac{1}{R_{0-1}} + \frac{1}{R_{1-2}} \right) V_1 + \frac{1}{R_{1-2}} V_2 = 0 \quad (20)$$

The foregoing equation is valid for the fictitious network in Figure 9A. It is easily seen that Equation 20 is valid for Figure 9 if we set $V_0 = V_s$ and $R_{0-1} \equiv \int_1^0 \frac{X_{s-1}}{A_1}$

All boundary points in steady state problems are handled in the foregoing manner.

D. The Computer Program

The computer program is set up to solve up to a 200 node, 3-dimensional network. The following information is supplied to the computer.

1. The resistivity of all materials (these may be functions of voltage).
2. The distance from the node of a segment to each of the six faces (the segment is considered to be a rectangular parallelipiped). (Irregular nodes can also be accommodated).
3. The cross-sectional current flow area in each direction away from the node.
4. Any contact resistances between segments.
5. Any boundary conditions imposed on the segments.

The computer checks the given data for discrepancies, computes the resistances between all the nodes and then solves for node potentials, subject to be given boundary conditions, by an iterative procedure.

BOUNDARY CONDITIONS

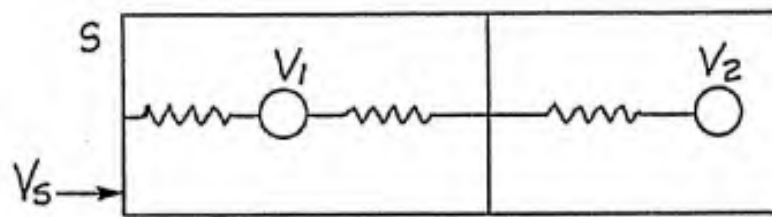


FIGURE 9

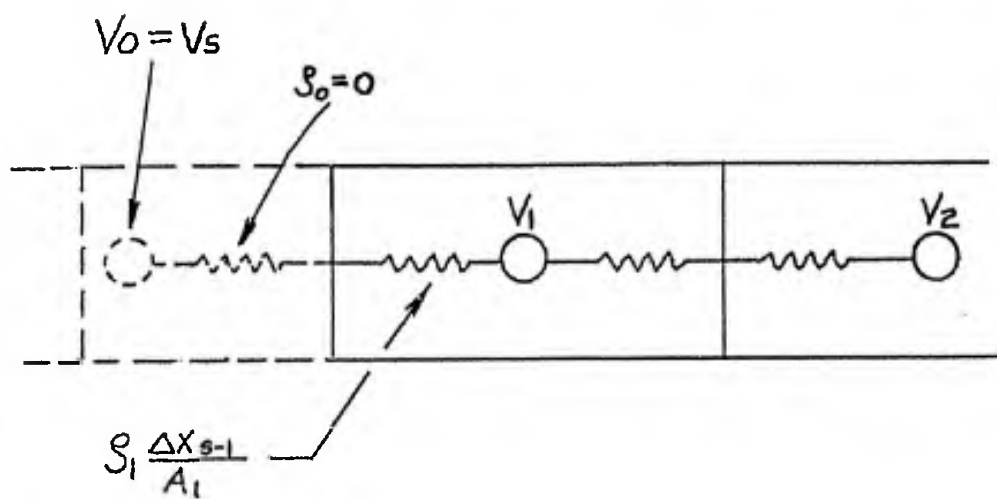


FIGURE 9A

E. Fuel Cell Application

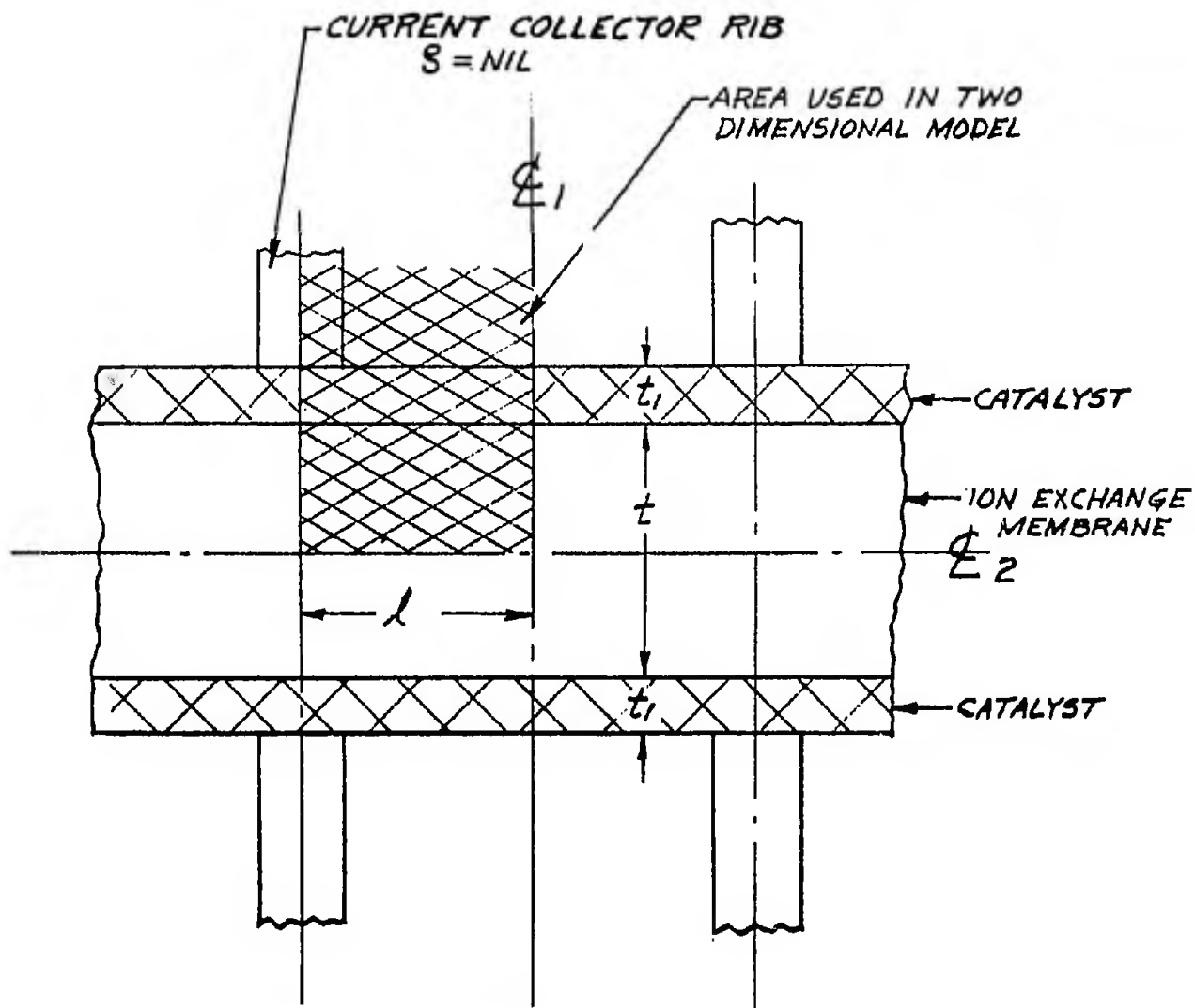
Let us estimate the effective resistance of the fuel cell geometry shown in Figure 10. Lines of symmetry show that it is sufficient to study the shaded area of Figure 10. The cell may be segmented as shown in Figure 11. The mesh shown in Figure 11 is fairly coarse, but is believed to give a good indication of the system characteristics. A finer mesh will, of course, give a numerically more exact answer.

The dimensions and resistances of the membrane and catalyst for a sample calculation are:

Membrane - = 27 ohm-cm
l = 0.4 inches
t = 0.0115 inches
depth b = 1 cm
Catalyst- = 0.3 ohms/sq.
l = 0.4 inches
t₁ = 0.003 inches
depth b = 1 cm

The potential at the membrane centerline was set as 1.0 volt. The collector potential was 0.5 volts. For a catalyst of zero resistance it is obvious that the potential at the membrane nodes will be 0.75 volts. The node potentials were calculated for the conditions given above:

Node 1	.7501
2	.7571
3	.7631
4	.7680
5	.7720
6	.7750
7	.7772
8	.7785
Average	$\frac{.7676}{8} = \bar{V}_m$



ALL CONTACT RESISTANCES = 0

FIGURE 10
 FUEL CELL GEOMETRICAL MODEL

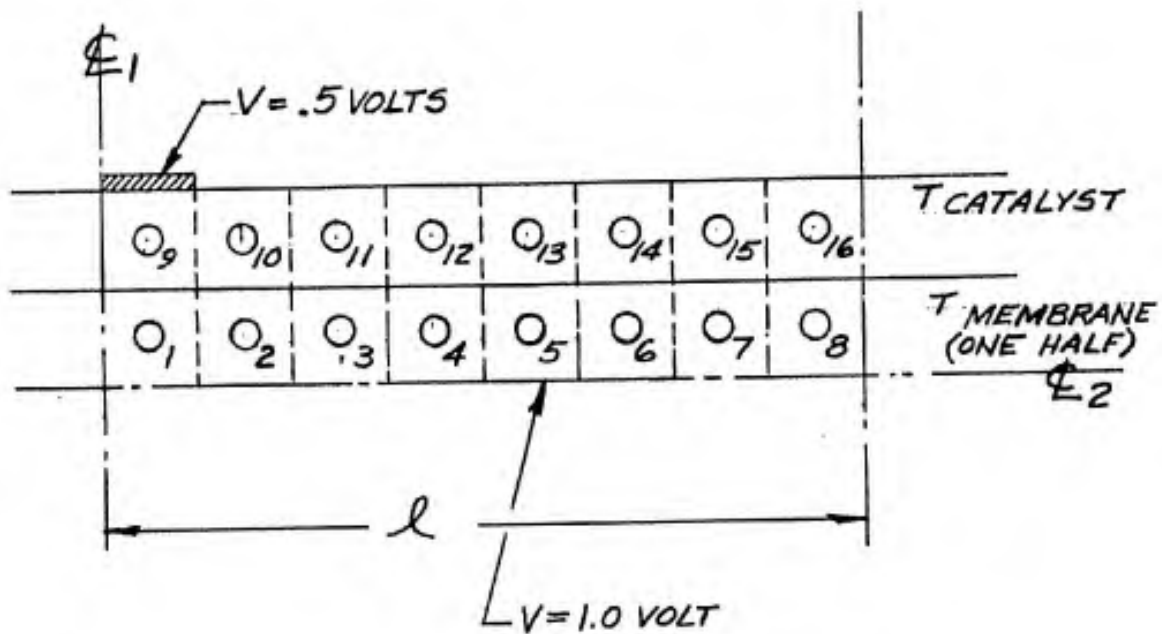


FIGURE 11
 NODE-REPRESENTATION OF FUEL-CELL MODEL

The average potential drop from the membrane centerline to the nodes is given by $V_{mc} - \bar{V}_m$, or 0.2323 Volts.

The ratio of the effective cell resistance R_{eff} (with a finite catalyst) to the cell resistance R_o (with no catalyst resistance) is simply:

$$\frac{R_{eff}}{R_o} = \frac{V_{mc} - V_{mo}}{V_{mc} - \bar{V}_m}$$

for the given problem this ratio is equal to

$$\frac{R_{eff}}{R_o} = \frac{.2500}{.2323} = 1.0757$$

$$\text{For catalyst} = 0 \quad V_{mc} - V_{\text{collector}} = I_o R_o$$

$$\text{For catalyst} \neq 0 \quad V_{mc} - V_{\text{collector}} = I R_{eff}$$

$$\text{Then } \frac{R_{eff}}{R_o} = \frac{I_o}{I}$$

$$\text{But catalyst} = 0 \quad V_{mc} - V_{mo} = I_o R_{mem}$$

$$\text{catalyst} \neq 0 \quad V_{mc} - \bar{V}_m = I R_{mem}$$

$$\text{Then } \frac{I_o}{I} = \frac{V_{mc} - V_{mo}}{V_{mc} - \bar{V}_m} = \frac{R_{eff}}{R_o}$$

The catalyst resistance adds about 7.5% to the basic cell resistance for the given geometry used here.

Thus, the above program will correlate the individual ohmic resistances and will allow prediction of cell assembly resistance.

Since the magnitudes of the individual ohmic resistances have been determined, it is hoped that by the next reporting period correlations will be completed to show relative contributions of such individual resistances. These will be checked with experimental measurements.

2.0 Task 1B Minimization of Electrolytic Losses

The method for correlating membrane constructions with total membrane ohmic resistance described in Progress Report Number 1 has been improved. This modified method relies on a plot of polymer-reinforcement resistance versus thickness to supply the individual component resistance. The individual components are then summed as in a series circuit to give total membrane resistance. Initial attempts to optimize the membrane reinforcing are described in the following parts in this report.

2.1 Investigate Resin Formulations

The investigation on this work problem will be initiated in December with the major part of the work completed before February. The work will be reported in Progress Report No. 3.

2.2 Effect of Membrane Thickness & Reinforcement on Cell Performance

A more thorough method has been devised for correlating cell construction with the ohmic resistance. In Progress Report Number 1 a method of calculating individual cloth-resin resistances and summing these as in a series circuit was presented. This method has been improved by determining the resistance versus thickness characteristics of membranes made from the reinforcements studies. The improved method decreased the average deviation between calculated and measured values by 50% (Progress Report Number 1, Pages 3-4, Table III).

Figure 12 shows this plot for non-woven Orlon fabric with a loading density of .055 grams/square inch and a Dacron-Ninon woven fabric with a loading density of 0.031 grams/square inch. Woven fabrics can be simply characterized by measuring the resistance of a membrane made from a single ply of the reinforcement. The characteristic fabric curve can then be drawn parallel to the ion exchange polymer curve through the single determined point. The curve may not, however, be extended lower than the original reinforcement thickness, or resistances rise very steeply with slight decreases in thickness. Another way of stating the above is by considering a membrane the exact thickness of the woven reinforcement. This membrane will have a characteristic resistance of R_m . If a new membrane is made of the same reinforcement but $2W$ inches thicker, it will essentially be a three ply membrane with W inches of ion exchange polymer present on either side of the reinforcement and in series with it. Thus, the new membrane will have a resistance of the first membrane plus $2W$ inches of ion exchange polymer on either side of it. Hence the resistance of these membranes are nearly linear with total thickness above the thickness of the cloth.

For non-woven reinforcements, the characteristic curve is a function of the density and type of material. As the membrane thickness increases, the membrane gradually approaches the resistance of the ion exchange polymer. With increasing density (decreasing thickness) the membrane resistance deviates from that of the pure polymer until it reaches a minimum, at which point the resistance increases sharply with small changes in thickness.

TABLE IV

See Table IV on following page.

TABLE IV

Cell	Thickness (Inches X 10 ³)	Calculated 1st Ply Resistance (OHM-CM ²)	Calculated 2nd Ply Resistance (OHM-CM ²)	Calculated 3rd Ply Resistance (OHM-CM ²)	Calculated Membrane Resistance (OHM-CM ²)	Measured Membrane Resistance (OHM-CM ²)	Percent Deviation
9-234*	34.5	2.30			2.30	2.16	+6.5
10-234	29.0	1.94			1.94	2.10	-7.6
11-234	19.0	1.48			1.48	1.43	+3.5
12-234	22.5	1.60			1.60	1.61	-
13-3ply 424*	17.0	2.77	2.77	2.77	8.33	8.33	-
14-3ply 424	14.0	3.60	3.60	3.60	10.80	10.70	-
43-3ply DN**	16.0	0.52	0.52	0.52	1.56	1.62	-3.7
45-3ply DN	26.0	0.76	0.76	0.76	2.28	2.53	-9.9
56-DN-234-DN	23.5	0.53	1.36	0.53	2.42	2.29	+5.7
57-DN-234-DN	29.0	0.53	1.49	0.53	2.55	2.68	-4.9
58-DN-234-DN	18.5	0.53	1.52	0.53	2.58	2.22	+16.2
59-234	27.5	1.82			1.82	2.16	-15.7
60-234	21.5	1.58			1.58	1.63	-3.1
61-234	18.0	1.42			1.42	1.63	-12.9
83-DN-234-DN	29.5	0.53	1.50	0.53	2.56	2.64	-3.0
84-234-424	30.0	1.68	2.70		4.38	5.25	-19.8
85-1/2 234-424-1/2 234	21.0	0.78	2.70	0.78	4.06	4.44	-8.6
86-1/2 234	29.0	2.27			2.27	2.47	-8.1
87-1/2 234-1/2 234	32.0	2.06	2.06		4.12	4.25	-3.1
88-234-234	33.0	1.41	1.41		2.82	2.85	-1.1
89-234-DN-234	32.0	1.35	0.53	1.35	3.23	3.59	-10.0
90-DN-1/2 234-DN	29.0	0.53	2.03	0.53	3.09	3.26	-5.2
91-DN-1/2 234-DN	22.0	0.53	2.40	0.53	3.46	3.47	-
92-1/2 234	22.0	2.03			2.03	2.11	-3.8
93-234-DN-234	26.0	1.39	0.53	1.39	3.31	2.87	+15.3
94-1/2 234	21.0	2.04			2.04	2.25	-
95-DN-234-DN	25.0	0.53	1.38	0.53	2.44	2.42	-

TABLE IV (Cont'd)

Cell	Thickness X (Inches X 10 ³)	Calculated 1st Ply Resistance (OHM-CM ²)	Calculated 2nd Ply Resistance (OHM-CM ²)	Calculated 3rd Ply Resistance (OHM-CM ²)	Calculated Membrane Resistance (OHM-CM ²)	Measured Membrane Resistance (OHM-CM ²)	Percent Deviation
BP-424-234-424	30.0	2.70	1.45	2.70	6.85	6.90	-
116-234-DN-234	26.0	1.38	0.53	1.38	3.29	3.50	-6.0
119-234-DN-234	26.0	1.38	0.53	1.38	3.29	2.94	+11.9
						Average	<u>6.5%</u>

24

LEGEND

- * 234 Types of cloth
- * 424
- ** DN - Dacron Ninon

RESISTANCE VERSUS THICKNESS OF IMPREGNATED REINFORCEMENTS

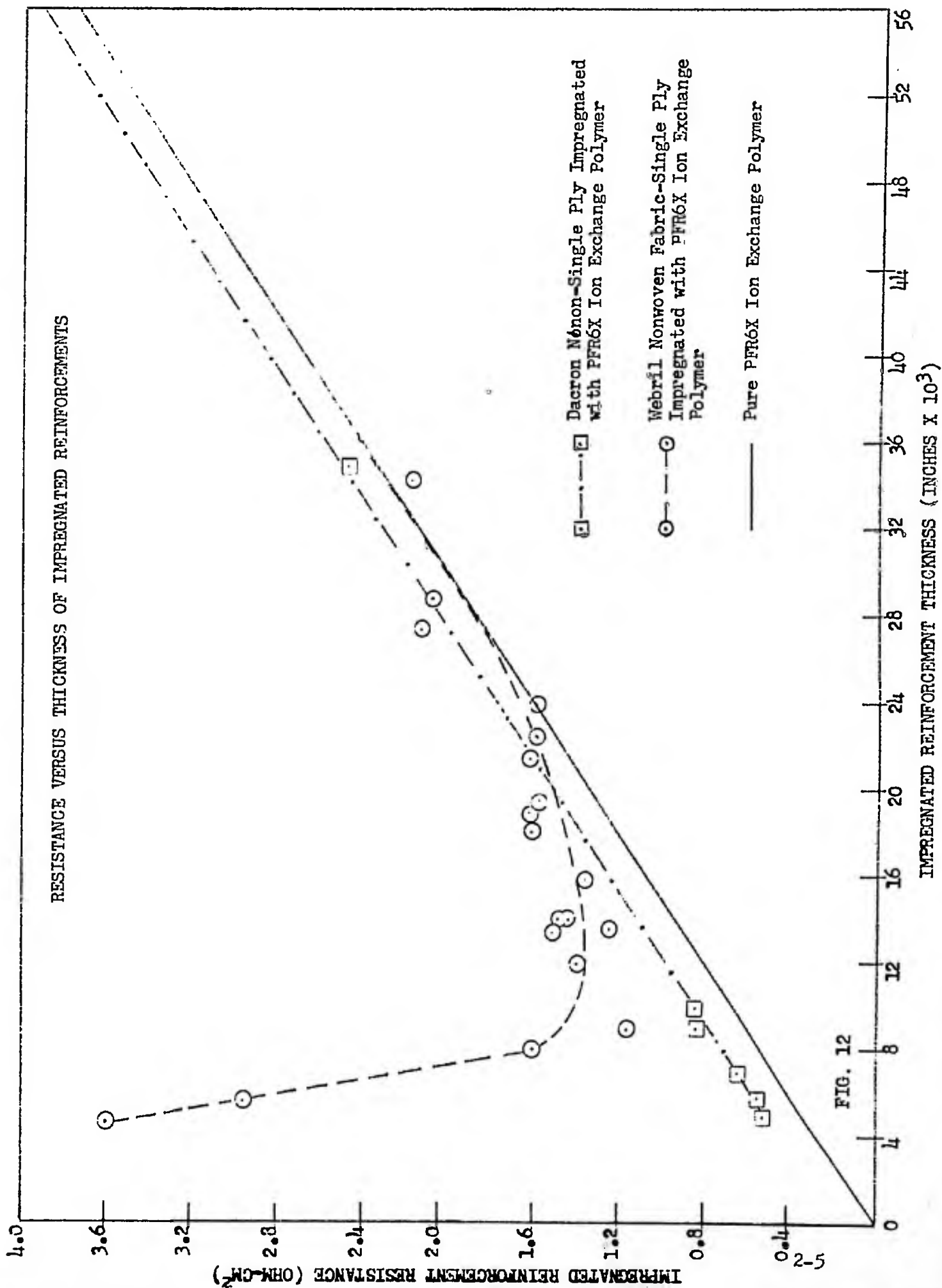


FIG. 12

IMPREGNATED REINFORCEMENT THICKNESS (INCHES X 10³)

IMPREGNATED REINFORCEMENT RESISTANCE (OHM-CM²)

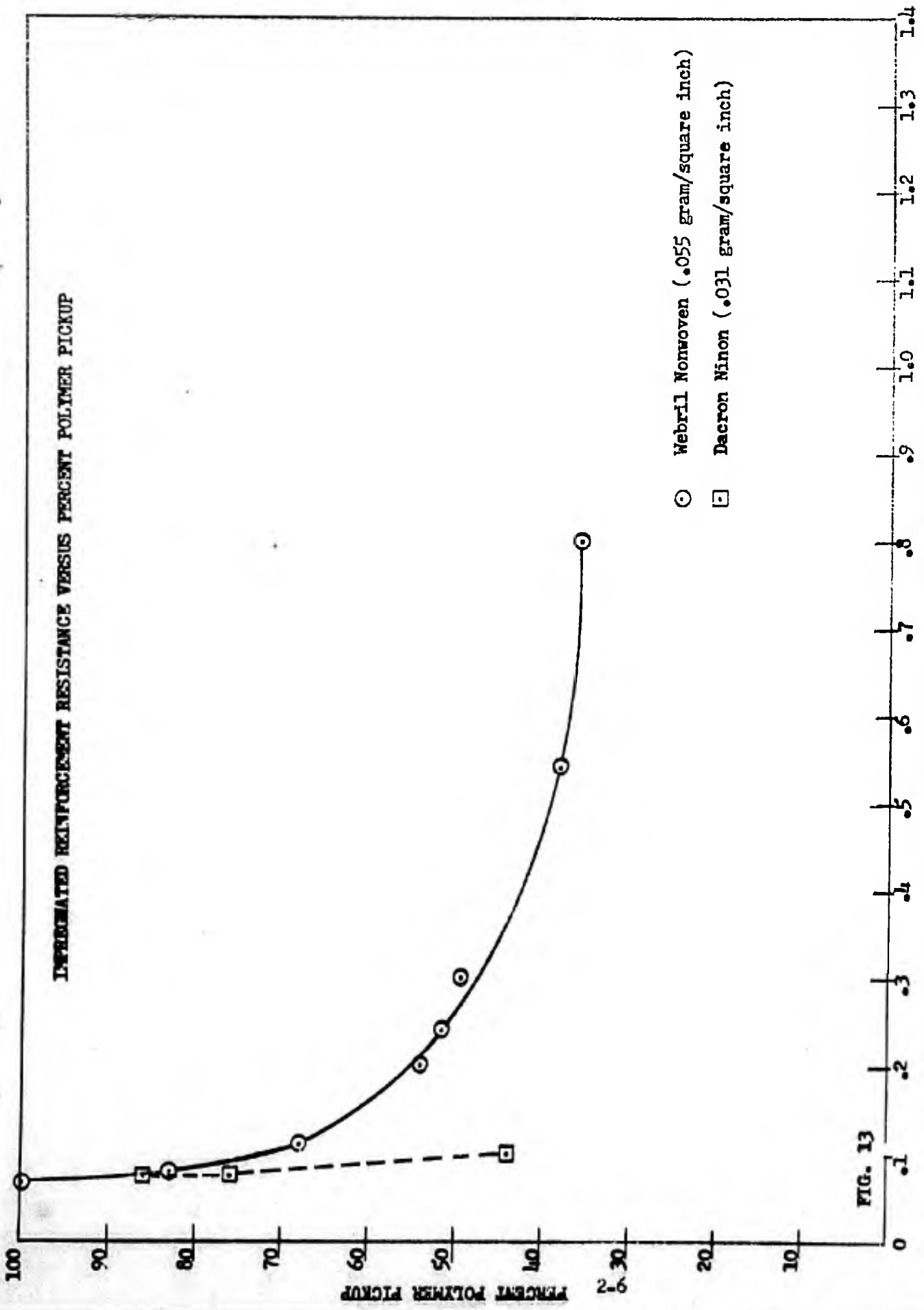
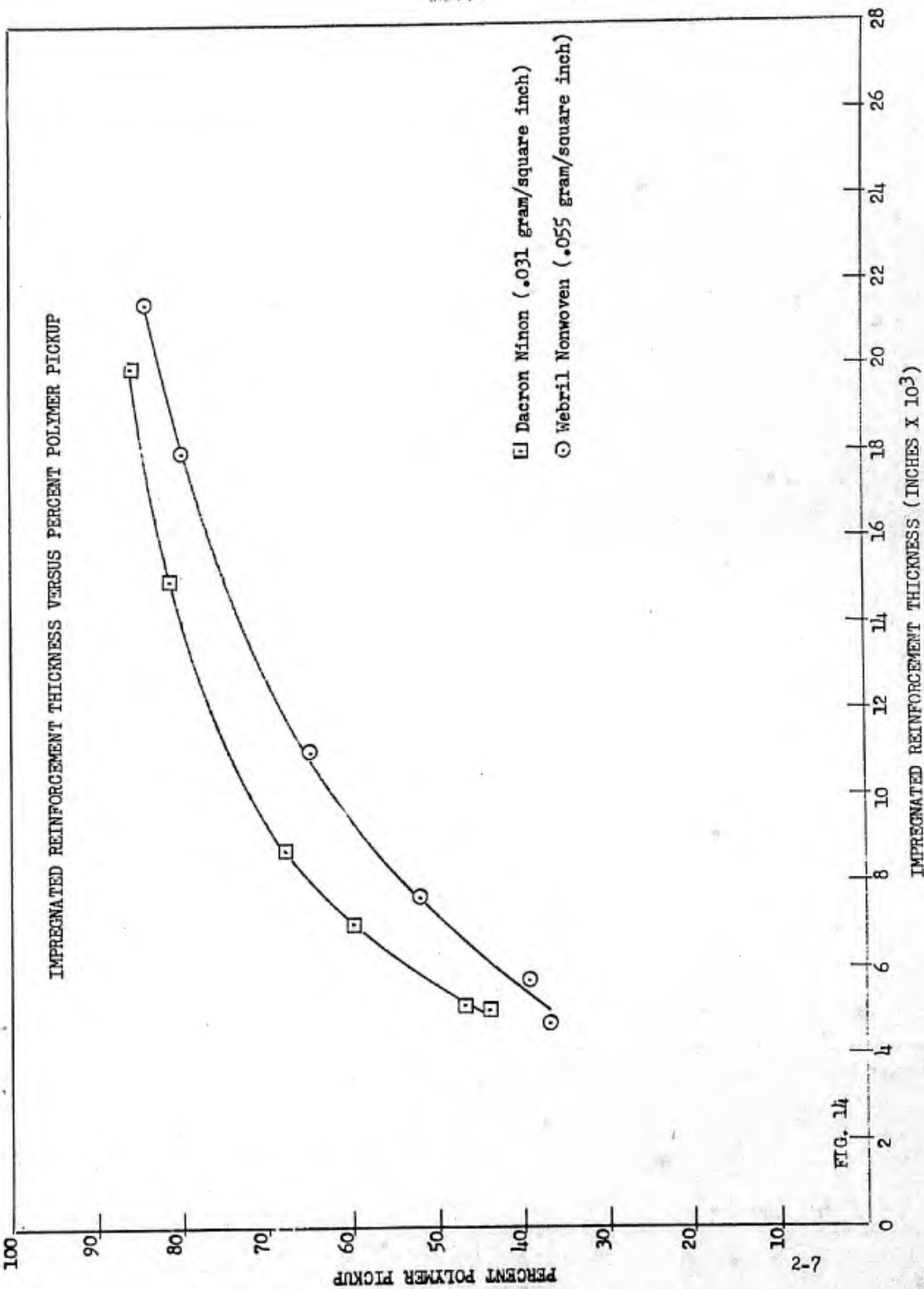


FIG. 13

RESISTANCE PER MIL THICKNESS (OHM-CM²/MIL)



□ Dacron Ninon (.031 gram/square inch)
 ○ Webril Nonwoven (.055 gram/square inch)

FIG. 14

The minimum is actually the point at which the percent polymer pickup * versus resistance slope changes abruptly (Figure 13). At this point, decreases in resistance due to decreased membrane thickness are smaller than increases in resistance due to lower resin pickup and the latter effect predominates.

For non-woven fabrics of the same density, but different initial thickness, a thickness relationship is used to determine the resistance versus thickness characteristic. For instance if the non-woven cloth was a double thickness of the cloth plotted in Figure 12, the resistance would be treated as the sum of two plies of the plotted cloth.

Thus, the procedure for predicting membrane resistance is to first characterize the resistance versus thickness characteristic of the reinforcement and then to treat each reinforcement as a series resistance (previously explained in Progress Report Number 1). Table IV shows predicted and experimentally determined values for the membranes made to date. Considering that the manufacturing method used only reproduces a given membrane to about 10%, the correlation seems to be well within this value for the most part. There are a few exceptions, but in general the correlations are much better than that offered in Progress Report Number 1.

2.3 Evaluation of Reinforcing Materials

Attempts to optimize the membrane reinforcement for other than ionic resistance have been preliminary to this date. The complete evaluation has been accomplished by three tests. The first is the determination of a membrane resistance. The second is the determination of the membrane strength by the Mullin-Burst apparatus. This apparatus consists of a hydraulically loaded diaphragm which is pressed against the clamped membrane. A gauge indicates the oil pressure required for the rubber diaphragm to puncture the membrane. The third test measures the ability of the membrane to withstand drying conditions while held in a clamped fixture. In this test, the membrane is mounted between two rigid frames with an open area of 4.0 inches by 4.0 inches. The corners of the frame are rounded to eliminate stress concentrations at this point. After mounting, the membrane is dried with a towel and allowed to sit at 40% RH. The time for the membrane to dry to a result of pinholing, cracking, or tearing is noted. Table V indicates the success attained to date with various combinations of reinforcements. Cell thickness is included as one of the criteria as this governs the cell weight which is critical in any optimization. During later reporting periods, a careful screening of all possible reinforcement materials will be initiated.

* Percent polymer pickup =
$$\frac{\text{wt. dried polymer} \times 100}{\text{wt. dried reinforcement} + \text{wt. dried polymer}}$$

It is planned to consider the following as possible reinforcements as well as the more common fabric materials:

1. Porous plastics.
2. Fiber glass cloths and mats.

The frame tests run to date indicate that the nature of the reinforcement should be such that the ion exchange polymer is supported nearly continuously throughout the membrane. Where the support is not continuous as in woven cloths, the polymer shrinks on drying, pulling away from the cloth and creating pinholes through the membrane. With non-woven fabrics, which are continuous throughout the polymer, failure never occurs by pinholing, but by cracking or tearing indicating lack of strength in non-woven materials. The low resistance requirement necessitates an 80% ion exchange polymer pickup by the reinforcing material. To date, the best compromise of these requirements has been combinations of woven and non-woven acid resistant cloth (Orlon or Dynel). It is possible that porous materials with at least 80% voids by volume may offer a solution.

TABLE V

Evaluation to date

Construction			Thickness Inches x 10 ³	Membrane Resistance OHM-CM ²	Mullin Burst psig	40% R.H. 4 x 4 Framed Dry Out Minutes
PLY 1	PLY 2	PLY 3				
DN**	234	DN	29.5	2.64	280	50
424*	234		30.0	6.08	110	55
½ 234*	424	½ 234	21.0	4.44	140	90
234	DN	234	32.0	3.60	285	55-150
DN	1½ 234	DN	29.0	3.26	340	50
DN	1½ 234	DN	22.0	3.50	340	45
1½ 234			18.5	2.11	80	30
DN	234	DN	25.0	2.42	300	20
424	234	424	30.0	6.90	265	200
1½ 234	1½ 234		32.0	4.25	250	200
234	234		33.0	2.74	130	45

Legend * 234
 * 424 Types of Cloth

** Dn - Dacron Ninon

3.0 Task IC - Minimization of Electronic Losses

The work on this problem will be initiated at a later date.

4.0 Task II - Internal Generation and Storage of Hydrogen
Fuel

4.1 Task IIA - Palladium and Other Absorbents for Hydrogen
This work will be accomplished by the General Electric
Heavy Military Electronics Department at Syracuse, New
York and will be reported under separate cover by the
above department.

4.2 Electrolyses by Ion Membrane Fuel Cells
Work to be initiated at a later date.

5.0 Task III - External Generation and Storage of Hydrogen and Oxygen

5.1 Electrolytic Methods

A sufficient number of engineering personnel have now been assigned for the accomplishment of this work. The first phase of this study on the design of an electrolytic generator will consist of a complete review of the literature in order to acquaint personnel with what has been accomplished, the current methods being used, and the application or adaptation of these and other ways for the electrolytic generation of H_2 and O_2 .

5.2 Chemical Methods

Hydride materials have been ordered and work started on this problem. A report will be submitted at the end of the next reporting period.

6.0

APPENDIX A

Photographs:

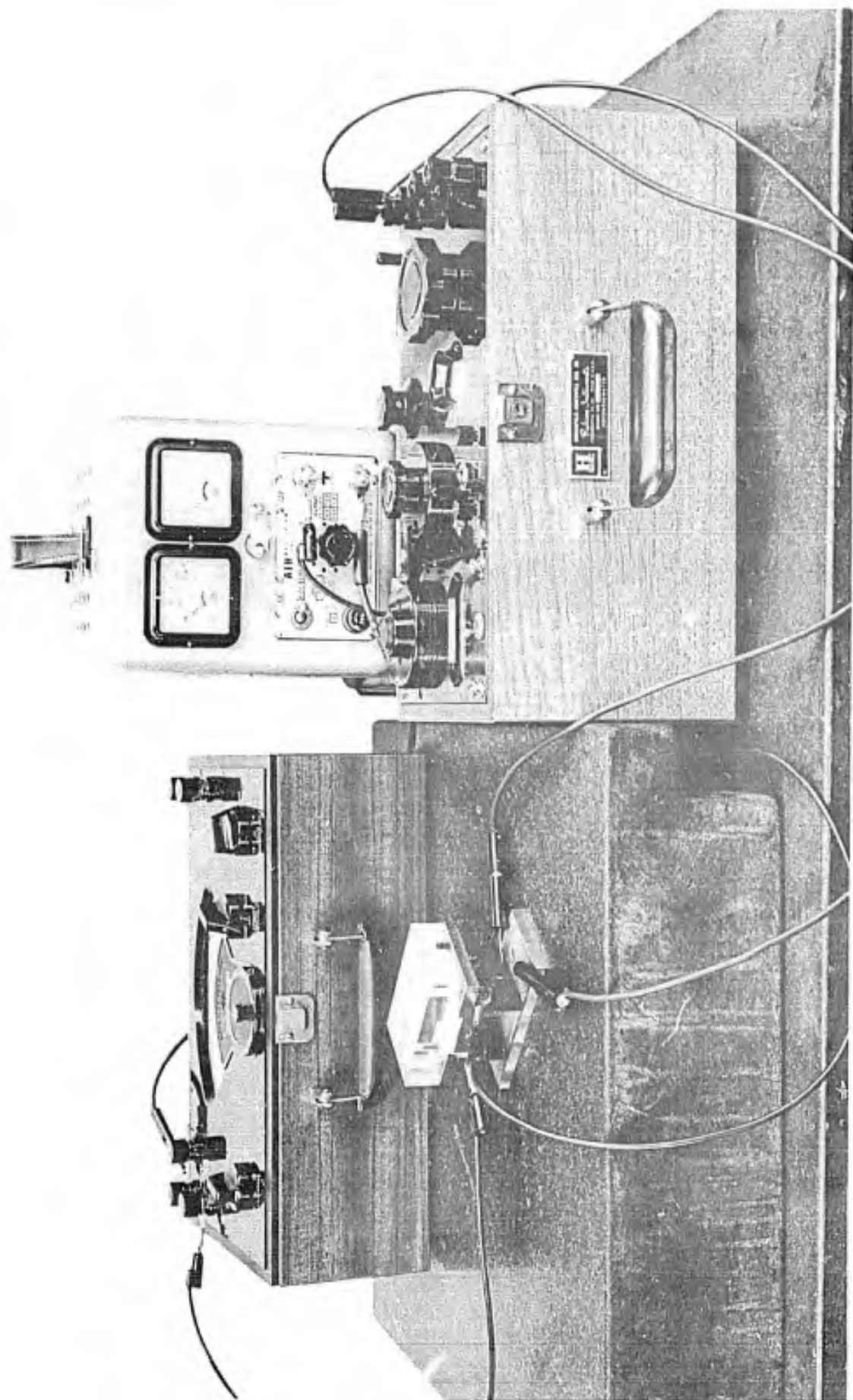
AAT 8388

Setup for Measurement of Contact Resistance

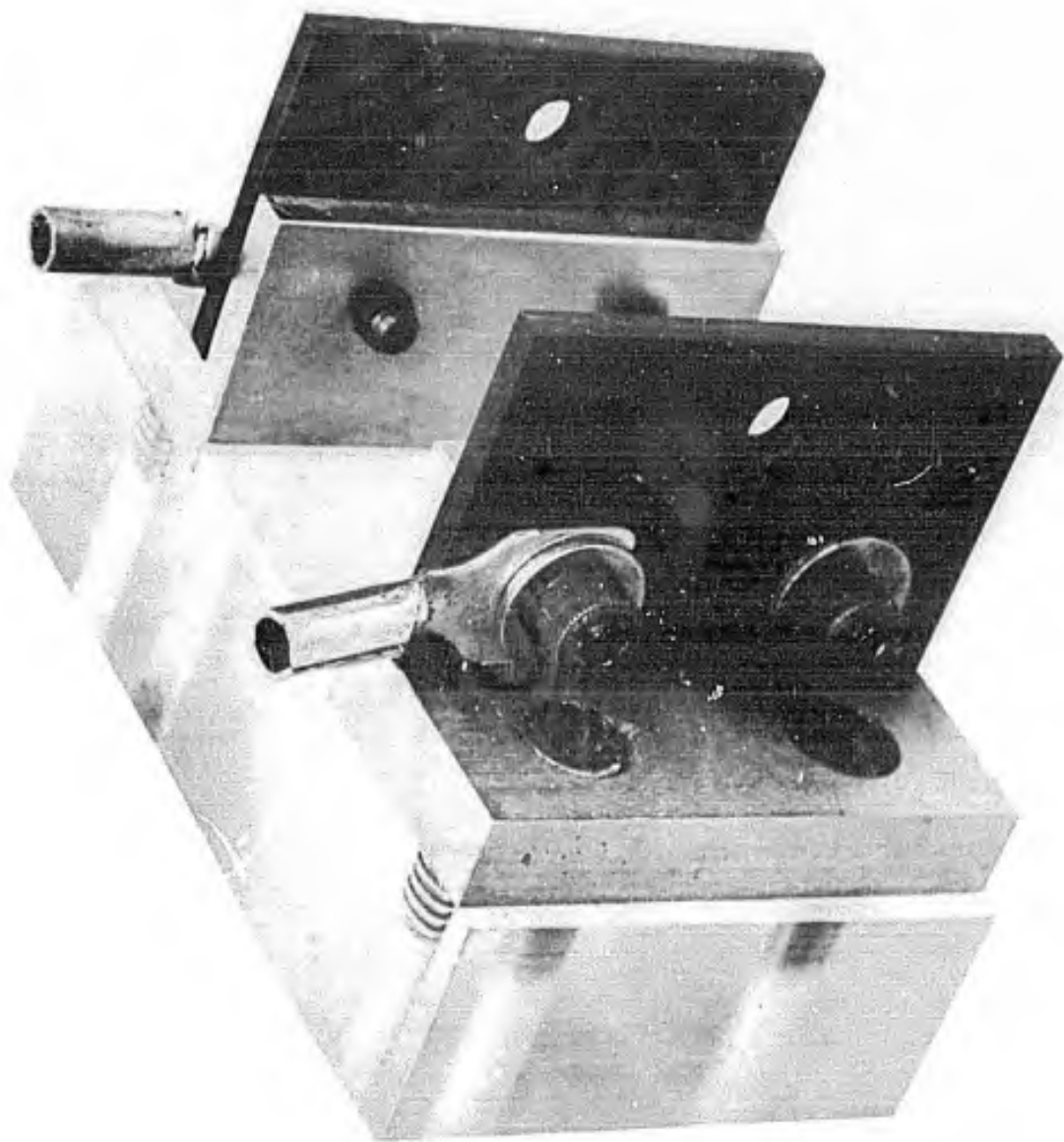
AAT 8389

Electrode Assembly for Contact Resistance

Measurements



AAT 8388



AAT 8389